International Journal of
Intelligent Systems and
Applications in Engineering
ISSN:2147-6799 www.atscience.org/IJISAE
Advanced Technology and Science
Original Research Paper

Artificial Neural Networks Approach for Earthquake Deformation Determination of Geosynthetic Reinforced Retaining Walls

Tahir Erdem Ozturk *[1]

Received 24th November 2013, Accepted 28th December 2013

Abstract: Back-to-back Mechanically Stabilized Earth (MSE) walls are commonly used for bridge approach embankments. Artificial Neural Network (ANN) analysis conducted in this study was applied for the first time in literature to estimate the seismic-induced permanent displacements of retaining walls under dynamic loads. For this purpose, a parametric study of seismic response analysis of reinforced soil retaining structures was performed to train the ANN using finite element analysis. The variables used to define wall geometry were reinforcement length, reinforcement spacing, wall height and facing type. The harmonic motion had three different levels of peak ground accelerations, namely 0.2g, 0.4g and 0.6g and had a duration of 6 sec with a frequency of 3 Hz. Although developing an analytical or empirical model is feasible in some simplified situations, most data manufacturing processes are complex and, therefore, models that are less general, more practical and less expensive than the analytical models are of interest. The agreement of the neural network predicted displacements and deformation classification with Finite Element Analyses results were encouraging by the means of correlation since the coefficient values of R=0.99 for ANN regression analysis were achieved.

Keywords: *Finite element analysis, Artificial neural network, Reinforced soil wall.*

1. Introduction

According to their economic advantages and superior engineering properties, construction of back to back mechanically stabilized earth (MSE) walls for bridge abutments are becoming more common throughout the world. Displacement based seismic performance studies of these structures have a vital role for the continuity of urban transportation after earthquakes. Although it is known that the seismic performance is related to wall geometry and earthquake characteristics, to gain better insight into mechanisms affecting the behaviour of these structures under dynamic loading conditions several engineering approaches are still being enhanced. The performance of MSE walls under seismic loading can be performed not only with physical testing methods (shaking table, centrifuge, full scale model) but also with analytical and numerical approaches which can be divided into pseudo-static (Monobe-Okabe) methods, displacement (Newmark) methods and finite element methods (FEM).

Finite element analysis is a preferred method because of its time and cost efficiency and holds much promise for simulating the behaviour of reinforced soil retaining structures under dynamic loading conditions. Especially for parametric studies that require large numbers of analysis, the validated FEM technique is preferred instead of time consuming and expensive physical tests. In this study Plaxis v.11.0, a popular FEM software program was used in the analysis of seismic response of reinforced soil walls. Geotechnical applications require advanced constitutive models for the simulation of the nonlinear and time dependent behaviour of soils. The modelling of the soil itself is an important issue; many geotechnical engineering projects involve the modelling of the structures and the interaction between the structures and the soil.

Although developing an analytical or empirical model is feasible, most numerical analysis data manufacturing processes are complex and, therefore, models that are less general, more practical and less expensive than the analytical models are of interest. An important advantage of using Artificial Neural Network (ANN) over regression in process modelling is its capacity in dealing with multiple inputs or responses while each regression model is able to deal with only one response. Another major advantage for developing ANN process models is that they do not depend on simplified assumptions such as linear behaviour or production heuristics. Neural networks possess a number of attractive properties for modelling a complex mechanical behaviour or a system: universal function approximation capability, resistance to noisy or missing data, accommodation of multiple nonlinear variables for unknown interactions, and good generalization capability. ANNs can efficiently be used as a tool for performing tasks such as function approximation (regression) and classification.

In the literature starting from 1990s, ANNs have been used productively for solving major particular problems in geotechnical engineering. Classical constitutive modelling is unable to imitate the situation of geomaterials because of formulation complexity, and undue empirical options. According to this, many researchers [2-21-22]; claimed that constitutive modelling is based on the elasticity and plasticity theoretician, and suggest neural networks as a dependable and practical disjunctive to modelling the constitutive monotonic and hysteretic behaviour of geomaterials.

To prevent damage caused by failure of soils as in liquefaction, there are different types of ANNs which take into account many applications in geotechnical engineering which include retaining walls ([6-12], dams [10], blasting [14], geo-environmental engineering [15], and tunnels and underground openings [4-18]. Ural and Saka [17]; Young-Su and Byung-Tak [19] also carried out studies to investigate the applicability of ANNs for predicting liquefaction.

[1] *Boğaziçi University, Turkey , * Email: erdemtahir@hotmail.com*

Goh et al. [6] developed a neural network model to provide initial estimates of maximum wall deflections for braced excavations in soft clay. The neural network was used to synthesize data derived from finite element studies on braced excavations in clay. The input parameters used in the model were the excavation width, soil thickness/excavation width ratio, wall stiffness, height of excavation, soil undrained shear strength, undrained soil modulus/shear strength ratio and soil unit weight. The maximum wall deflection was the only output.

Table 1. Comparison of neural network prediction and field measurements [6]

Case History	Measured wall deflection (mm)	Predicted wall deflection (mm)
Laveder (Singapore)	32	31
Laveder (Singapore)	36	28
Telecom (Singapore)	56-84	65
Vaterland 3	76	76
NGI (1962)	114-140	107
San Fransisco	20-60	59
Mana (1977)	72-150	122

2. Theory and Methodology

2.1. Artificial Neural Networks

Zurada [23] and Fausett [5] explained that ANNs consist of a number of artificial neurons known as 'processing elements' (PEs), 'nodes' or 'units'. For multilayer perceptrons (MLPs), which are the most commonly used ANNs in Geotechnical engineering, processing elements are situated as an input layer, an output layer and one or more intermediate layers called hidden layers (Fig. 1).

The dissemination of data in MLPs begins at the input layer where the input data are submitted. During the process each input is weighted, summed and elapsed through a transfer function to make the nodal output. If the network cannot find a set of weights that perform the input-output mapping, it will be still regulating its weights on presentation of a set of training. This process is called ‘learning’ or 'training'.

Since the training set of a model has been finished effectively it must be validated. The aim of validation is to check the capacity of the model to generalize the limits set by the training data. If this type of procedure is appropriate, the model is considered robust enough to be generalized.

The coefficient of correlation, r, the root mean squared error, RMSE, and the mean absolute error, MAE, are the main criteria that are often used to evaluate the prediction performance of ANN models. The coefficient of correlation, a value defined between 0.0 and 1.0, is a measure that is used to determine the relative correlation and the goodness-of-fit between the predicted and observed data.

The objective of the linear regression model is to find the unknown function f, which relates the input variable x to the output variable y. The function f can be obtained by changing the slope tanφ and intercept β of the straight line in Fig. 2.a, so that the error between the actual outputs and outputs of the straight line is minimized. The same principle is also used in ANN models. ANNs can form the simple linear regression model by having one input, one output, no hidden layer nodes and a linear transfer function (Fig. 2.b). The connection weight w in the ANN model is equivalent to the slope tanφ and the threshold θ is equivalent to the intercept β, in the ANN linear regression model.

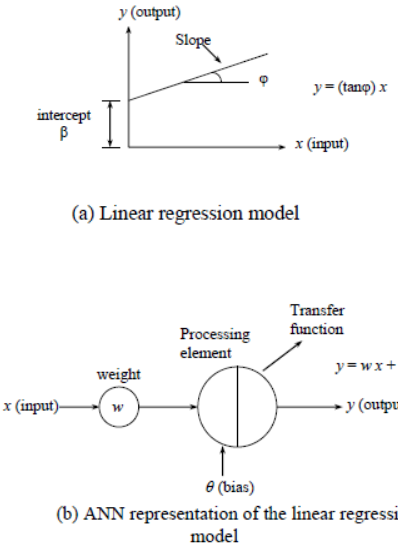

Fig. 2. Linear regression versus ANN models [5].

It is known from previous studies [7] that the peak ground acceleration and the wall displacements are not linearly related. When there are non-linear problems, ANNs can deal with these by changing the transfer function or network structure, and the type of non-linearity can be replaced by changing the number of hidden layers and the number of nodes in each layer.

2.2. Strong Ground Motion and Intensity Measures

In estimating strong-motion characteristics for seismic design, there is a need to define the parameters that reflect the destructive potential of the motion. Providing quantitative estimates of expected levels of seismic ground-motion requires characterizing the complex nature of strong-motion accelerograms by using simple parameters and the development of predictive relationships for these parameters.

The main elements of earthquake engineering field and structural dynamics are ground motion time history records of acceleration, velocity and displacement. Among the information included in time history record, amplitude, frequency content and duration characteristics of the strong ground motion are the most crucial ones for engineering purposes [11]. Several ground motion parameters have been defined in the literature and are listed as follows; peak ground acceleration (PGA), peak ground velocity (PGV), effective peak acceleration (EPA), arias intensity (AI), cumulative absolute velocity (CAV), acceleration spectrum

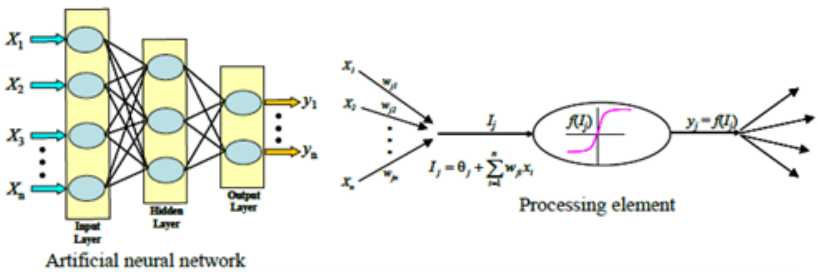

Fig. 1. Typical structure and operation of ANNs [23].

intensity (ASI), and velocity spectrum intensity (VSI).
In this study SeismoSignal, software used to process strong motion data, was utilized to determine all these IM's from acceleration time history for three different harmonic motions that are varied with respect to PGA values. This software comprises an efficient and simple way to process strong-motion data, featuring a user-friendly visual interface and the capability of deriving a number of strong-motion parameters.
Uang and Bertero [16] examined the adequacy of the parameters that have been used to identify the damage potential of an earthquake and reported that the destructiveness of a ground motion record at the foundation of a structure relies on the intensity, frequency content, duration and the dynamic characteristics of the structure. They reached the conclusion that the most dependable parameter for measuring the damage potential is earthquake energy input.

3. CALCULATIONS

3.1. Numerical Model with FEM

In this study, Plaxis, an extensively used finite element program was utilized for the numerical analysis. Two dimensional (2-D) plane strain analysis was performed during the study.
As can be seen from Fig. 3, the boundary conditions were identified as fixities; at the bottom boundary total fixity was identified which means both horizontal (u_x) and vertical (u_y) are zero. Below the wall level at the right and left boundaries of the basement only horizontal fixities were assigned.

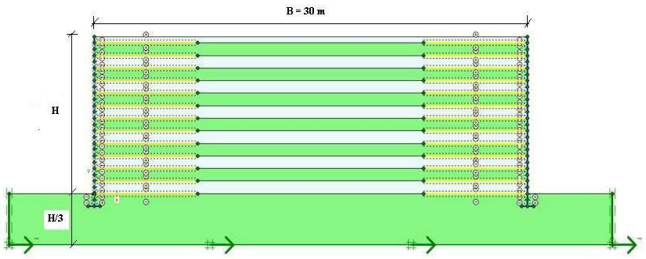

Fig. 3. The geometry of the back to back wall model

The absorbent boundaries were used in dynamic calculations to account for the fact that in reality soil is semi-infinite medium. Although these boundaries also affect the wall displacements, without these boundaries the waves would be reflected from the model boundaries, returning into the model and disturbing the results. To avoid these spurious results reflection absorbent boundaries were specified at the bottom right and left side boundary. In order to minimize absorbent boundary effects on wall displacements, the back to back retaining wall was used as the most adaptable and realistic design. The geometry of these FEM models was defined as in all models the width (B) was fixed at 30 m. and the height of the wall (H) got values between 5m and 10m. Below the ground level one concrete panel or one modular block was embedded as a foundation.
The linear elastic perfectly-plastic Mohr-Coulomb Model (MCM) model was used to define the backfill soil. The model involves five input parameters, E and υ for soil elasticity; φ and c for soil plasticity and ψ as an angle of dilatancy and the values were assigned as stated in Table 2.

Table 2. Material properties of soil

Material Model	Unit Weight (γ_{dry})	Elasticity Modulus (E)	Poisson Ratio (ν)	Cohesion (c)	Internal Friction Angle (ϕ)	Dilatancy Angle (Ψ)
Mohr-Coulomb	18 kN/m^3	30000 kN/m^2	0.3	5 kN/m^2	35°	0°

The reinforcing elements used to define geotextiles could only sustain tensile forces and have no bending stiffness. For modelling elastoplastic behaviour, the maximum tension force in any direction is bound by Np. For geotextile reinforcements EA=4,000 kN/m was chosen for elastic axial stiffness and NP=400 kN/m for 10% strain condition.
In our parametric analysis, modular block facing and precast concrete panel were used as facing elements. The modular block facing elements were modelled as 0.5 m in width and 0.25 m in height and linear elastic material model was selected to define the material with properties; unit weight (□dry) was 21 kN/m3, elastic modulus (E) was 4.4x106 kN/m2 and Poisson ratio (ν) was 0.17.
Precast facing panels were modelled using plates of 0.60 m of width and height and 0.20 m of thickness. The material properties were defined as 23.5 kN/m3 for unit weight, 25x106 kN/m2 for elastic modulus, 0.20 for Poisson ratio and 28 MPa for 28-day compressive strength. Based on these properties, the axial stiffness EA was calculated as 5,000,000 kN/m. Bending stiffness EI was found as 16,660 kNm2/m and finally, for one meter height, the weight of the panels was found to be equal to 4.7 kN/m/m.
The connection between facing panels is modelled by some researchers by simple hinges and the compressibility that develops between them due to the presence of pads is neglected. Since deformations are the main outcome of this study, instead of hinges rubber bearing pads were modeled using the same type of elements that were used for the facing panels.

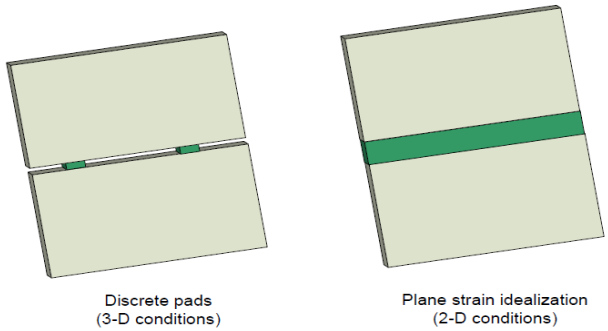

Fig. 4. Modeling of discrete bearing pads in plane strain analysis.

Taking into account the cross sectional area of the rubber pad, which is 0.0085 m2, the axial stiffness is equal to 400 kN/m. However, this refers to one pad with dimensions 100 mm * 85 mm * 60 mm. In plane strain analysis illustrated in Fig. 4, the pad was replaced by a plate whose equivalent axial stiffness was calculated as 533.3 kN/m. Knowing the thickness of the pads (d = 0.085 m), the bending stiffness per linear meter was found equal to 0.321 kNm2/m. Note that pads are assumed to be weightless and to have a very high Poisson's ratio of 0.495.
In the present finite element model, elements were placed between the precast concrete panel and the backfill soil interface. The interfaces were also placed between all modular block elements. The strength reduction factor value was chosen as 0.7 between backfill soil and precast concrete panel and between modular blocks.
The Finite Element Model was subjected to a base excitation, which is a variable amplitude harmonic motion. The prescribed displacement feature of the program at the base of the wall was

employed to assign the constant frequency cyclic load. The cyclic load was applied at equal time intervals of 0.05 s and its variation with time is shown in Fig. 5. This accelerogram has been accepted as a good representation of commonly encountered accelerograms [3]. The peak amplitude of the input acceleration was selected as 0.2, 0.4 and 0.6 g. A frequency of 3 Hz was selected to represent a typical predominant frequency of medium to high frequency content earthquake.

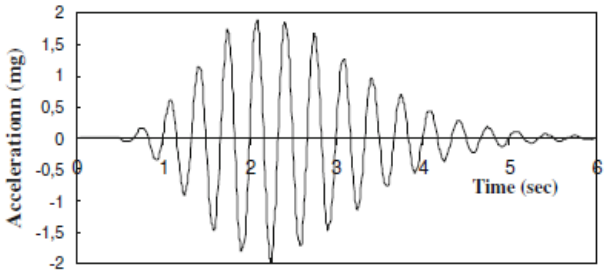

Fig. 5. Base harmonic acceleration history used as cyclic load in the analysis (apeak=0.2g).

3.2. Validation Analysis of Numerical Model

In order to validate the finite element modeling technique under earthquake loading conditions, the results of a shaking table test reported by Ling et al. [13] were used and the results were compared and reported by Guler et al. [7].

To check the accuracy of the Finite Element Model (FEM) used in this study, results of a 1-g shaking test reported by Anastasopoulos et al. [1] were modeled using the same Finite Element modeling technique.

Anastasopoulos et al. [1] performed tests on back to back retaining walls. The configuration details of model setup are shown in Fig. 6. Two different steel wire meshes were used in order to simulate flexible and stiff reinforcements. Plane strain idealization of discrete reinforcement elements was used in order to transform 3-D conditions of physical test to a 2-D finite element model according to the study of Zevgolis [20]. After this adjustment, the elastic axial stiffness parameters which were required for numerical analysis were calculated as EA = 400 kN/m for stiff and 40 kN/m for flexible reinforcement.

The facing panels were made of *t*=2 mm Plexiglas strips (E = 3 GPa), and were connected to each other through a customized connection using a "shear key" configuration to block relative horizontal displacements between consecutive panels but allowing differential rotation (as in reality). Based on these properties, the axial stiffness EA was calculated as 6,000 kN/m. Bending stiffness EI was found as $2x10^{-3}$ kNm^2/m. Poisson's ratio and unit weight of Plexiglas strip facing were assigned as 0.37 and 0.0234 kN/m/m respectively for numerical analysis.

The backfill consisted of dry "longstone" sand, a very fine and uniform quartz sand industrially produced with adequate quality control. Test model was constructed with D_r = 44% to represent the loose state (Table 3).

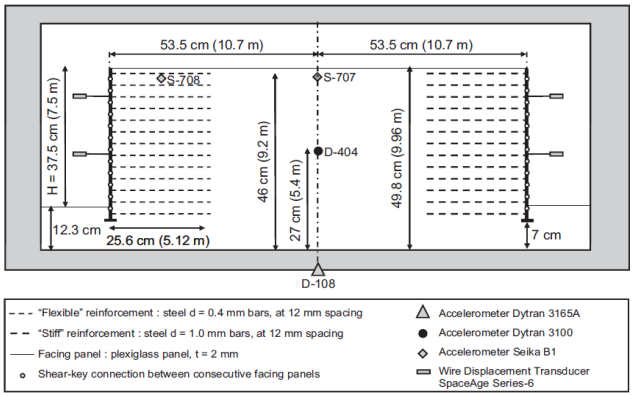

Fig. 6. Shaking table model setup showing geometry and instrumentation. [1]

Table 3. Longstone sand index properties of validation model. [1]

Specific gravity (G_s)	2.64
Maximum void ratio (e_{max})	0.995
Minimum void ratio. (e_{min})	0.614
Median diameter (D_{50}) (mm)	0.15
Uniformity coefficient, (C_u)	1.42
Unit weight (kN/m^3)	18
Friction Angle (φ)	36°
Relative Density (D_r)	44%
Poission Ratio (υ)	0.3
Dilation Angle (ψ)	6°

The model was subjected to an "extreme seismic shaking 60-cycle cos sweep" of dominant period T_o=0.5 s and PGA= 1.0 g (Fig. 7).

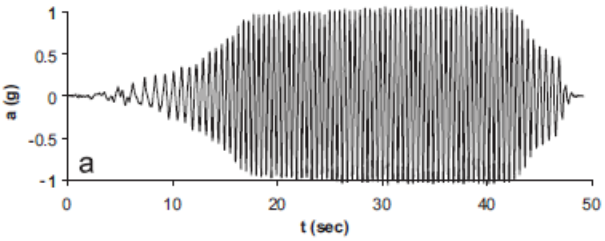

Fig. 7. 60-cycle "extreme shaking" synthetic excitation [1].

Although not realistic (both in terms of retained soil density and shaking intensity), this test was conducted to derive deeper insights on the ultimate capacity of reinforced soil walls.

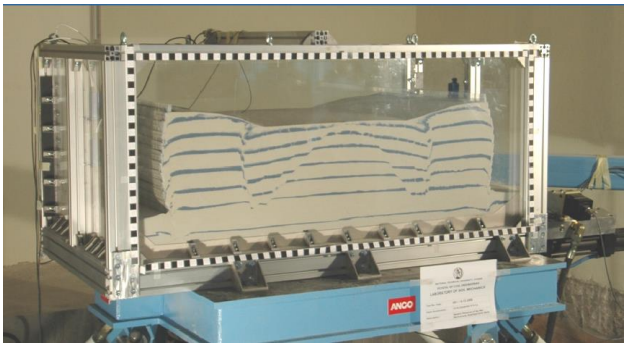

Fig.8. Shaking table test results after harmonic motion. (60-cycle "cos sweep" of dominant period T_o=0.5 s and PGA= 1.0 g) [1].

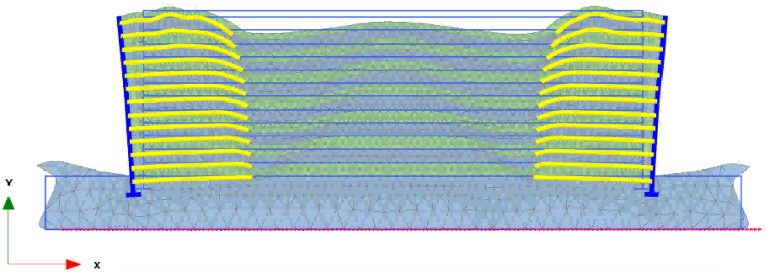

Fig. 9. Plaxis output after harmonic motion. (60-cycle "cos sweep" of dominant period T_0=0.5 s and PGA= 1.0 g).

Fig. 8 shows the final position of the wall after 60-cycle "cos sweep" seismic excitation which has a period T_0=0.5 s and PGA= 1g. Fig. 9. shows the Plaxis models final deformation position.

The order of shaking events started with smaller intensity records, followed by the larger ones, and completed with multi-cycle artificial motions: the two 30-cycle so-called "cos sweeps" of PGA=0.5 g and To=0.4 or 0.8 s.

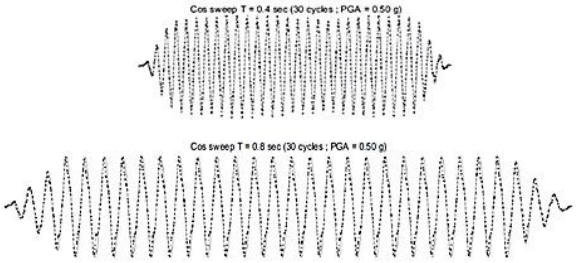

Fig. 10. Multi-cycle accelerograms used as seismic excitations [1].

The results of the numerical analyses are summarized in Fig. 11 and Fig. 12. The results of FEM model are compared directly with shaking table test results to serve as validation of the numerical analysis and of the Mohr Coulomb model.

As depicted in Fig. 11 and Fig. 12 the numerical prediction (analysis of shaking table model) compares well with the results of the shaking table tests for the two artificial 30-cycle cos-sweeps. The numerical analysis underestimates the cyclic component of the horizontal (lateral) wall displacement, but the examined herein (reinforcement stiffness and dominant period of residual displacement.

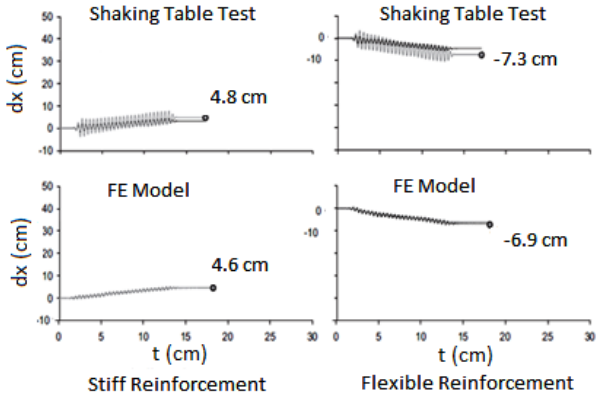

Fig. 11. Wall displacement time histories for the multi-cycle seismic excitation of T=0.4 s

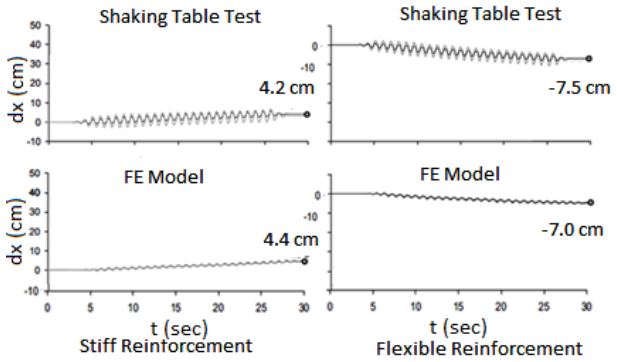

Fig.12. Wall displacement time histories for the multicycle seismic excitation of T=0.8s

3.3. ANN Analysis

In this study, twelve input and one output parameters were used in order to predict the permanent displacement of back to back retaining walls. Five of them were about wall geometry illustrated in Fig. 13 as; wall height (H) varied between 5m and 10m, reinforcement length (L), length over height ratio (L) changed between 0.5 and 2, vertical spacing of reinforcement (Sv) varied between 0.2m and 0.8m, facing type (modular block and precast concrete panel).

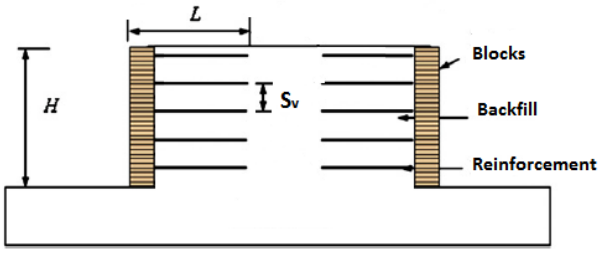

Fig. 13. Back to back retaining wall geometry.

The other seven parameters were about intensity measures of dynamic loading as PGA (m/s2), PGV (m/s), EPA (m/s2), AI (m/s), CAV (m/s), ASI (m/s), VSI (m). The program Seismosignal was used to obtain the intensity measure results for a given acceleration time history. Table 4. gives the results of three harmonic ground motion analyses.

Table 4. Seismosignal results of harmonic motion.

Harmonic Ground Motion	PGA (m/s^2)	PGV (m/s)	EPA (m/s^2)	AI (m/s)	CAV (m/s)	ASI (m/s)	VSI (m)
0.2g	1,977	0,096	1,961	0,5	2,826	2,014	0,317
0.4g	3,999	0,196	3,903	2,151	5,962	4,098	0,644
0.6g	5,93	0,288	5,882	4,505	8,48	6,041	0,95

ANN was initially trained using a set of experimental data obtained from the computer simulations of FE models of the back to back wall and this set of data was called training data. Design of ANN

architecture consists of determining the number of layers, the number of neurons in each layer, activation functions of the neurons and the learning algorithm for the network. The most common ANN architecture is a multi-layer feed-forward structure also known as a multilayer perceptron (MLP) trained by Back-Propagation (BP) algorithm [9]. There are three different types of layers in a MLP: an input layer representing the input design variables, an output layer representing the response, and a number of hidden layers that perform the mapping of the input data before they enter the output layer. (Fig. 14)

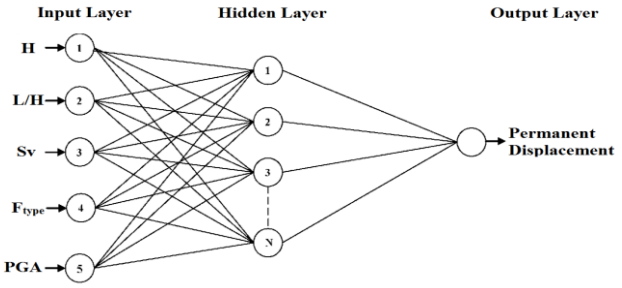

Fig. 14. Multi-layer perceptron (MLP) with three layers.

Other than the training data, validation data were used during the learning process. The learning halts when the error of the validation data falls below a threshold value or when a maximum number of iterations (epochs) is reached. Finally, the performance of the network was estimated using independent test data that had not been used in the learning process. The mean square error (MSE) is generally used for calculating the error. For this study, the Levenberg-Marquardt (LM) algorithm was adopted for its efficiency in training MLP. The details of the back propagation (BP) algorithm can be found in the literature [8].

4. RESULTS

4.1. Finite Element Analysis Results

Fig. 15 shows deformed models lateral displacement $|u_x|$ after seismic loading by the means of shadings. Color scale on the right side of deformed model shows the displacement distributions of all systems.

Walls with modular block facing and precast concrete panel facing have different displacement increments behaviour as can be seen from Fig. 16 and Fig. 17. Also it was obtained from figures that in both facing types the permanent displacements increased nonlinearly with increasing PGA values. It was observed that this increase was more obvious at higher walls for example for a 9 meter wall the permanent displacements were 17, 28 and 32 cm for 0.2, 0.4 and 0.6 g PGAs respectively. As an example, for a 5 meter wall the permanent displacement values did not vary so much with increasing PGA. This on the other hand shows that the relation between permanent displacements and wall height is also non-linear.

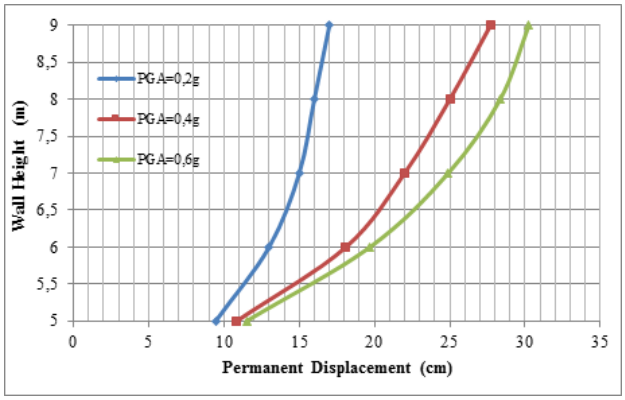

Fig. 16. Permanent displacement according to wall height (L/H= 0.7, S_v =40cm, modular block facing).

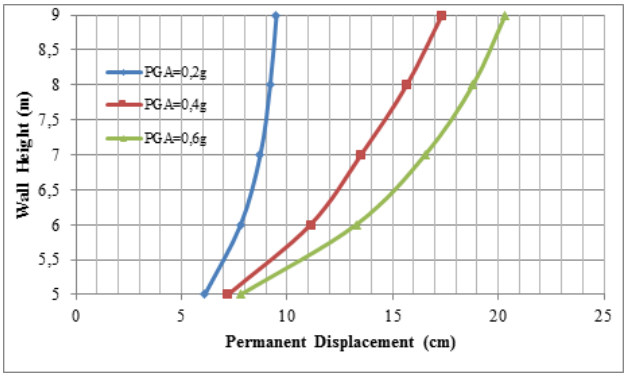

Fig.17. Permanent displacement according to wall height (L/H= 0.7, S_v =40cm, precast concrete panel facing).

Relative displacement δr is the ratio of maximum displacement to wall height. Fig.18 shows the variation of δr values for L/H ratios for a wall model example where Sv=0.4m and H=7m obtained from FEM analysis. It can be observed that the relative displacements increased nonlinearly with increasing PGA and the differentiation was more obvious between L/H ratios of 0,7 and 1. Especially for a PGA of 0.2g it is also clearly seen that the

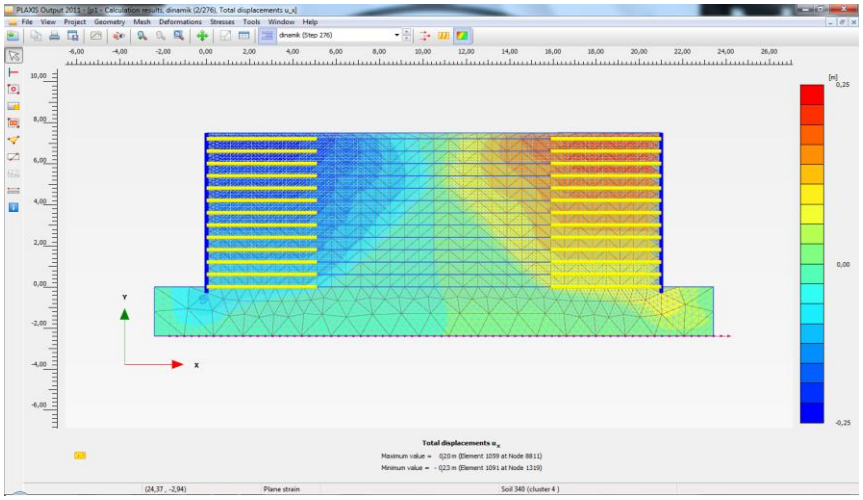

Fig. 15. Deformed mesh after seismic loading (PGA= 0.2g).

relationship between relative displacement and L/H ratio is also non-linear.

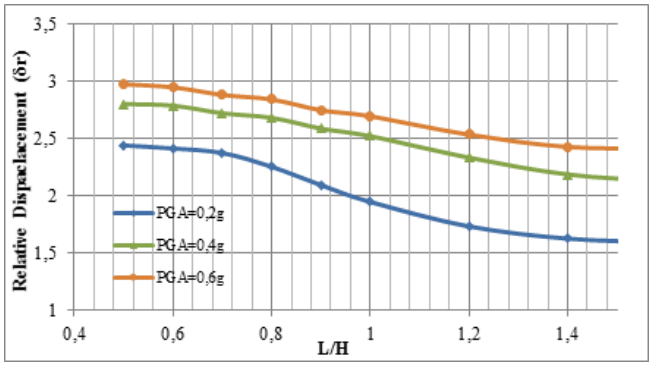

Fig.18. Relative displacement factors according to L/H. (Sv=40 cm, H=7m)

As can be seen in Fig.19 displacement values normalized by height are increased with increasing vertical spacing between reinforcements.

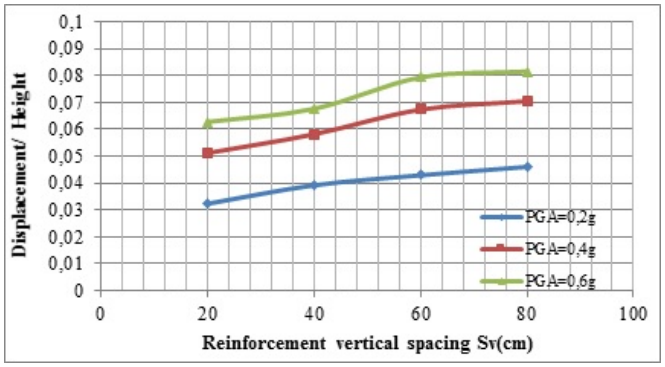

Fig. 19. Displacement / Height according to vertical spacing Sv. (L/H=0.7 H=7 m).

4.2. ANN Regression Analysis Result

Squared Error (MSE) is performance metric adopted to determine the network performance, while regressions; R is used to measure the correlation between outputs and targets. The fitting curve between targets with inputs is shown in Fig.20 and the best validation performance is approached at epoch 10.

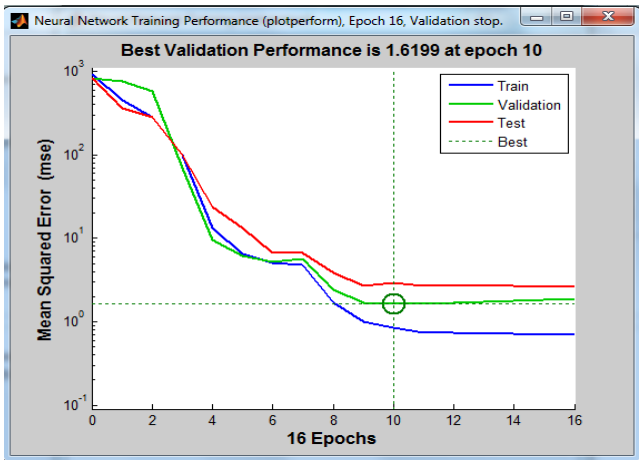

Fig. 20. Validation performance.

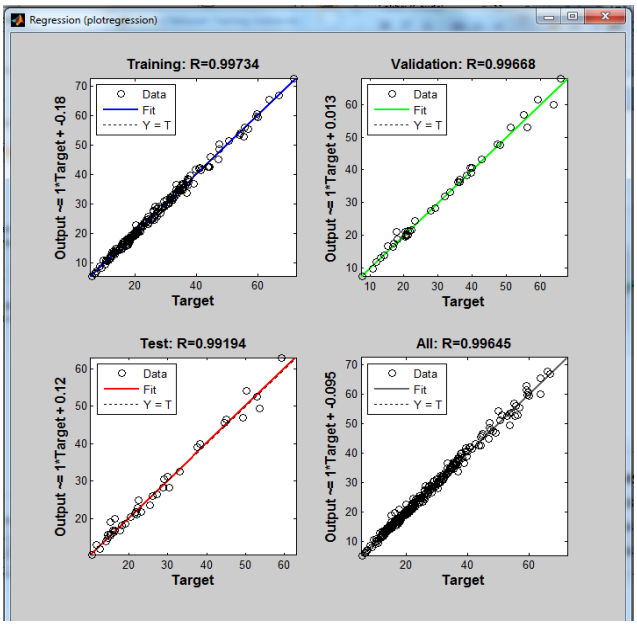

Fig. 21. Fitting curve between targets with inputs.

The neural network is trained and validated using the first batch of 110 learning points and the performance is evaluated using 83 test points. The performance of the ANN regression model for the first 83 learning points using 10 neurons in the hidden layer can be seen in Fig. 21. Even for a relatively low number of learning points, ANN regression performs well on the test data. Totally 276 data are distributed between training, validating and testing in different percentages. Despite distribution of the data in various proportions, no significant change about R has been seen in Table 5.

Table 5. Results for MSE and regression for Different data distribution.

	Number of Samples	MSE	R
Training	110	0,8412	0,9972
Validating	83	60,033	0,9871
Testing	83	35,156	0,9902

	Number of Samples	MSE	R
Training	220	17,781	0,9951
Validating	28	22,581	0,9932
Testing	28	22,096	0,9921

The same geometric input with each intensity measures gives high coefficients of correlation for testing data as seen in Table 6. It is assumed that this result was obtained because a harmonic motion was used in this study.

Table 6. Search for each IM input features.

Number of Features	R (%)	Intensity Measures
1	99.37	PGA
2	98.32	PGV
3	99.24	EPA
4	98.84	AI
5	98.75	CAV
6	99.23	ASI
7	99.42	VSI

The agreement of the neural network predicted displacements and FEA results were encouraging, as shown in Table 7.

Table 7. Comparison of neural network predictions and FEA results.

H (m)	S_v (m)	L/H	Facing type	PGA	Measured displacement (cm)	Predicted Displacement (cm)
5	0,4	1,4	Modular Block	0,6 g	18,2	18.12
6	0,2	0,5	Modular Block	0,4 g	31,09	29.52
6	0,4	1,2	Modular Block	0,4 g	27,1	26.38
7	0,6	1	Modular Block	0,2 g	23,7	23.25
7	0,8	0,7	Concrete Panel	0,6 g	41	39,8
8	0,2	0,7	Modular Block	0,2 g	24,8	25,6
9	0,4	1	Concrete Panel	0,4 g	32	32,7

5. CONCLUSION

In the numerical analysis part of the study permanent displacements of back to back reinforced segmental retaining walls under earthquake loading condition were calculated with the finite elements program Plaxis. Three harmonic motions which have PGA values 0.2g, 0.4g and 0.6g respectively with a frequency of 3 Hz were performed.

The investigated parameters such as height of the wall, type of facing (modular block and concrete panel), reinforcement length and spacing of reinforcement led to the following results. The permanent displacement increased with the height of the wall. Permanent displacements of modular block facing walls were more than precast concrete panel facing. Increasing reinforcement length decreased the permanent displacements of wall facing and maximum tensile stress on reinforcement. Decreased reinforcement vertical spacing (Sv) caused a reduction on the permanent displacements of wall facing. The peak ground acceleration had strong influence on the dynamic response of the walls. As an example, when the peak ground acceleration was 0.2g, 0.4g, and 0.6g permanent displacements for a wall with 9m height were 17cm, 28cm, and 32cm, respectively. It can be seen that peak ground acceleration and permanent displacements were correlated nonlinearly. Also the permanent displacement and L/H ratio correlation was nonlinear.

The study intended to use the ANN model in order to make reliable predictions for geosynthetic reinforced wall design and to check whether the results of finite element analysis results fall between reasonable limits.

The ANN was used to synthesize data derived from finite element studies on back to back geosynthetic reinforced retaining walls under seismic excitation. The input parameters used in the model were H, L, L/H, Sv, Ftype, PGA, PGV, EPA, AI, CAV, ASI, and VSI. The permanent displacement of the wall was chosen the only output.

The important point of the seismic evaluation of the seismic response of the back to back MSE retaining wall is the selection of ground motion intensity measure IM for different earthquakes. In this study due to constant frequency (3 Hz) value of harmonic motions with different PGAs (0.2g, 0.4g and 0.6g), intensity measures; PGV, EPA, CAV, ASI, and VSI are linearly correlated with PGA values but AI is not. Therefore any of these IMs is enough to approach high coefficients of correlated ANN model.

Using ANN regression analysis, the scatter of the predicted ANN displacements relative to the displacements obtained using the finite element method were assessed. The results produced high coefficients of correlation for training and testing data of 0.997 and 0.989, respectively. So, the agreement of the neural network predicted displacements and deformation classification with Finite Element Analyses results were encouraging by the means of correlation since the coefficient values of R=0.99 for ANN regression analysis were achieved.

References

[1] Anastasopoulos I., T., Georgarakos, V., Georgiannou, V., Drosos, R., Kourkoulis, 2010, "Seismic performance of bar-mat reinforced-soil retaining wall: Shaking table testing versus numerical analysis with modified kinematic hardening constitutive model", Soil Dynamics and Earthquake Engineering, 10.1016/j.soildyn.2010.04.020 journal homepage: www.elsevier.com/locate/soildyn

[2] Basheer, I.A., 2002, "Stress-strain behavior of geomaterials in loading reversal simulated by time-delay neural networks", Journal of Materials in Civil Engineering, 14(3), 270273.

[3] Bathurst, R.J., Hatami, K., 1998, "Seismic response analysis of a geosynthetic-reinforced soil wall", Geosynthetics Internatinal, 5(1-2):127-166.

[4] Benardos, A.G. and D.C., Kaliampakos, 2004, "Modeling TBM performance with artificial neural networks", Tunneling and Underground Space Technology, 19(6), 597-605.

[5] Fausett, L.V. 1994, "Fundamentals neural networks: Architecture, algorithms,and applications", Prentice-Hall, Englewood Cliffs, New Jersey.

[6] Goh, A.T.C., K.S., Wong and B.B., Broms, 1995, "Estimation of lateral wall movements in braced excavation using neural networks", Canadian Geotechnical Journal, 32, 1059-1064.

[7] Guler, E., E.Cicek M., Hamderi, M.M., Demirkan, 2011, "Numerical analysis of reinforced soil walls with granular and cohesive backfills under cyclic loads", Bull Earthquake Eng.DOI 10.1007/s10518-011-9322-y

[8] Haykin, S.S., 1999, Neural networks: a comprehensive foundation. Upper Saddle River, N.J., Prentice Hall.

[9] Kim, D.H., D.J., Kim, et al., 1999, "The application of neural networks and statistical methods to process design in metal forming processes", International Journal of Advanced Manufacturing Technology 15(12): 886-894.

[10] Kim, Y. and B., Kim, 2008, "Prediction of relative crest settlement of concrete-faced rockfill dams analyzed using an artificial neural network model", Computers and Geotechnics, 35(3), 313-322.

[11] Kramer, S.L., 1996, Geotechnical Earthquake Engineering, Prentice Hall, New Jersey.

[12] Kung, G.T., E.C., Hsiao, M., Schuster and C.H., Juang, 2007, "A neural network approach to estimating deflection of diaphram walls caused by excavation in clays" Computers and Geotechnics, 34(5), 385-396.

[13] Ling, H.I., Y., Mohri, D., Leshchinsky, C., Burke, K., Matsushima, H., Liu, 2005 "Large-scale shaking table tests on modular-block reinforced soil retaining walls", J Geotech Geoenviron Eng ASCE 131(4):465-476

[14] Lu, Y. 2005, "Underground blast induced ground shock and its modeling using artificial neural network", Computers and Geotechnics, 32(3), 164-178.

[15] Shang, J.Q., W., Ding, R.K., Rowe and L., Josic, 2004, "Detecting heavy metal contamination in soil using complex permittivity and artificial neural networks", Canadian Geotechnical Journal, 41(6), 1054-1067.

[16] Uang, C.H. and V.V., Bertero, 1988, Implications of recorded earthquake ground motions on seismic design of buildings structures, UCB/EERC-88/13, California.

[17] Ural, D.N. and H., Saka, 1998, "Liquefaction assessment by neural networks", Electronic Journal of Geotechnical Engineering, http://www.ejge.com/Ppr9803/ Ppr9803.htm

[18] Yoo, C. and J., Kim, 2007, "Tunneling performance prediction using an integrated GIS and neural network", Computers and Geotechnics, 34(1), 19-30.sa

[19] Young-Su, K. and K., Byung-Tak, 2006, "Use of artificial neural networks in the prediction of liquefaction resistance of sands", Journal of Geotechnical and Geoenvironmental Engineering, 132(11), 1502-1504.

[20] Zevgolis, I., 2007, "Numerical and Probabilistic Analysis of Reinforced Soil Structures", PhD Thesis, Purdue University.

[21] Zhu, J.H., M.M., Zaman and S.A., Anderson, 1998a,

"Modeling of soil behavior with a recurrent neural network", Canadian Geotechnical Journal, 35(5), 858-872.

[22] Zhu, J.H., M.M., Zaman and S.A., Anderson, 1998b, "Modeling of shearing behavior of a residual soil with recurrent neural network", International Journal of Numerical and Analytical Methods in Geomechanics, 22(8), 671-687.

[23] Zurada, J.M., 1992, Introduction to artificial neural systems, West Publishing Company, St. Paul.

International Journal of
Intelligent Systems and
Applications in Engineering
ISSN:2147-6799 www.atscience.org/IJISAE
Advanced Technology and Science
Original Research Paper

Matlab's GA and Optimization Toolbox: A Fourbar Mechanism Application

L.C. Dülger*[1], H. Erdoğan [2], M.E. Kütük[1]

Received 8th November 2013, Accepted 14th January 2014

Abstract: This study presents an optimization approach for synthesis of planar mechanisms. A four bar mechanism is chosen for an application example. This mechanism is studied with the constraints assigned. Genetic Algorithm (GA) is applied during optimization study. GA in Optimization Toolbox is then compared with nonlinear constrained numerical optimization command; fmincon in Matlab©. Different case studies are performed by considering different target points. These mechanisms are drawn using Excel© spread sheet to see their animations. An optimization example is presented here. Performances of both algorithms are then compared in terms of coupler curves precision points. Their use in designing a four bar mechanism is explored for its further use.

Keywords: *Four bar mechanism, Mechanism synthesis, Optimization, Genetic algorithm.*

1. Introduction

The purpose of this study is to perform a comparative study on synthesis of mechanical linkages using genetic algorithm. Some recent studies on the subject covering more than ten years are surveyed. Since the optimum synthesis of a mechanism requires a repeated analysis to find the best possible one to meet requirements, dimensional synthesis will be preferred here. A simulation study will be performed on a four bar linkage. The linkage parameters will be tabulated as a guide for the user. The computational synthesis methods are also applied [1, 2, 3]. The science of motion is related with the analysis and synthesis of mechanisms in study of Kinematics. It also deals with the relative geometric displacements of points and links of a mechanism. Dimensional Synthesis looks for determining optimal dimensions of a prescribed type of mechanism. The type and dimensional levels are the main factors in the mechanisms for the study of kinematic synthesis of mechanisms [4-8].

The objective is to apply an evolutionary method for synthesis of planar mechanisms and present a design guide for its use in linkage mechanisms. The evolutionary process is not related with the results which are obtained from enumeration of mechanisms. Some algorithms are included in Matlab as toolbox facility. This study is organized as follows; first part outlines an introduction with synthesis of planar mechanism, statement of problem. Literature survey is also given on mechanism synthesis using GAs. Matlab Optimization Toolbox is introduced with Genetic algorithm Toolbox. Some illustrative examples are done on optimization based synthesis problems for 4 bar mechanism. An example application is given by using two optimization approach based on Matlab environment. Matlab Optimization Toolbox with constrained optimization is compared with Genetic Algorithm Toolbox (GA).

[1] *Gaziantep University, Faculty of Eng., Mech. Eng. Dept., Gaziantep/TURKEY*
[2] *Turkish Railway Corporation, Adana/TURKEY*
** Corresponding Author: Email: dulger@gantep.edu.tr*

2. Survey on Synthesis on Planar Mechanisms

Many studies are seen on optimization based synthesis and optimization using GAs. They are included in the following part, and appeared with the years where the studies were performed [9-11].S. Hoskins and G.A Kramer have previously introduced use of ANNs with optimization techniques (Levenberg-Marquardth Optimization) to synthesize a mechanical linkage generating a user-specified curve [12]. M.H.F.Dado and Y.S.Mannaa have described the principles for an automated planar mechanism dimensional synthesis, [13]. R.C. Blackett has presented a technique for the optimal synthesis of planar five link mechanisms in Master's Study [14]. P.S. Shiakolas et al. have presented representative examples utilizing Matlab through a web browser interface [15]. J. A Cabrera et al. have dealt with solution methods of optimal synthesis of planar mechanisms [16]. R. Bulatovic and S.R Djordjevic have performed optimal synthesis of four bar linkage by method of controlled deviation with Hooke-Jeeves's optimization algorithm [17]. Laribi et al. have proposed a combined Genetic algorithm- Fuzzy Logic Method (GA-FL) to solve the problem of path generation in mechanism synthesis [18]. K.G. Cheetancheri et al. have presented a study on Computer Aided Analysis of Mechanisms Using Ch Excel, [19]. J.F. Collard et al. have presented a simple approach to optimize the dimensions and the positions of 2D mechanisms for path or function generator synthesis [20]. H.H. Cheng et al. have presented a study on a web-based mechanism analysis and animation [21]. J. Xie et al. have proposed an approach to kinematics synthesis of a crank rocker mechanism. Coupler link motions passing from a prescribed set of positions are generated [22]. Liu et al. has presented a new approach using the framework of genetic algorithms (GAs) [23]. S .Erkaya and İ. Uzmay have presented a study on dimensional synthesis for a four bar path generation with clearance in joints [24]. N.N. Zadeh et al. have used hybrid multi-objective genetic algorithms for Pareto optimum synthesis of four-bar linkages. Objective functions are taken tracking error (TE) and transmission angles deviation (TA) [25]. S.K. Archaryya et al. have performed

a study on performance of Evolutionary Algorithms (EAs) for four-bar linkage synthesis. Three different evolutionary algorithms such as GA, Particle Swarm Optimization (PSO), differential Evolution (DE) have been applied for synthesis of a four bar mechanism [26]. A. Kentli et al. have presented a study on genetic coding application (GCA) to synthesis of planar mechanisms [27]. K. Sedlaczek and P. Eberhard have presented a study on extended Particle Swarm Optimization technique based on the Augmented Lagrangian Multiplier Method [28]. F. Pennunuri et al. have given optimal dimensional synthesis for planar mechanisms using differential evolution (DE) with four examples, Pennunuri et al. [29]. Erdogan has performed a comparative study on GA and fmincon for planar mechanisms in his thesis. A four bar mechanism is analysed. [30].

3. Motion, Path and Function Generation

The dimensional synthesis problems can be broadly classified as motion generation, path generation and function generation [1-3].
(i) Motion Generation: a rigid body has to be guided in a prescribed manner in motion generation. Motion generation is related with links controlling the links in the plane. The link is required to follow some prescribed set of sequential positions and orientations.
(ii) Path Generation: If a point on floating link of the mechanism has to be guided along a prescribed path, then such a problem is classified as a problem of path generation. Path Generation controls the points that follow any prescribed path.
(iii) Function Generation: The function parameters (displacement, velocity, acceleration etc.) of the output and input links are to be coordinated to satisfy a prescribed functional relationship. The Function Generation is related with functional relationship between the displacement of the input and output links [23].

3.1. Four Bar Mechanism

A four bar mechanism has four revolute joints that can be seen with numerous machinery applications. There is a relationship of the angular rotations of the links that is connected to the fixed link (correlation of crank angles or function generation). If there is not any connection to the fixed link which is called the coupler link. This position of the coupler link can be used as the output of the four bar mechanism. The link length dimensions determine the motion characteristics of a four bar mechanism according to the Grashof's theorem. The link lengths are the function of the type of motion and are identified for a four bar chain as follows [2]. Here l is the longest link length, s is the shortest link length, p and q are the two intermediate link lengths. The input-output equation of a four bar is taken as by looking at link lengths. Figure 1. shows all possible mechanism configurations as crank rocker, double rocker and double crank.

4. Kinematics of Four Bar Mechanism

The kinematic analysis of a four-bar mechanism is considered first. Figure 2 shows four bar mechanism in general coordinate system [16, 26]. The design procedure of a four-bar linkage starts with the vector loop equation referring to Figure 2. The position vectors are given as $\vec{R}_1, \vec{R}_2, \vec{R}_3, \vec{R}_4$. The offset angle is notated by θ_0 and the input angle is θ_2. The position vectors are used to get complete four bar linkage as in Eqn.(1).

$$\vec{R}_2 + \vec{R}_3 = \vec{R}_1 + \vec{R}_4 \tag{1}$$

The complex number notation can be substituted next by using scalar lengths of the links as r_1, r_2, r_3 and r_4. It is given in Eqn. (2)

$$r_2 e^{i\theta_2} + r_3 e^{i\theta_3} = r_1 e^{i\theta_0} + r_4 e^{i\theta_4} \tag{2}$$

Here θ_3 and θ_4 the angles to be found. They can be expressed as

$$\theta_3 = f\{r_1, r_2, r_3, r_4, \theta_2, \theta_0\} \text{ and}$$

$$\theta_4 = f\{r_1, r_2, r_3, r_4, \theta_2, \theta_0\} \tag{3}$$

Eqn. (2) is expressed with its real and imaginary parts with assumption of θ_0=0, then the real and imaginary parts are written as in Eqn's (4.1) and (4.2)

$$r_2 \sin\theta_2 + r_3 \sin\theta_3 = r_4 \sin\theta_4 \tag{4.1}$$

$$r_2 \cos\theta_2 + r_3 \cos\theta_3 = r_1 + r_4 \cos\theta_4 \tag{4.2}$$

$$K_1 \cos\theta_3 - K_4 \cos\theta_2 + K_5 = \cos(\theta_2 - \theta_3) \tag{5.1}$$

$$K_1 \cos\theta_4 - K_2 \cos\theta_2 + K_3 = \cos(\theta_2 - \theta_4) \tag{5.2}$$

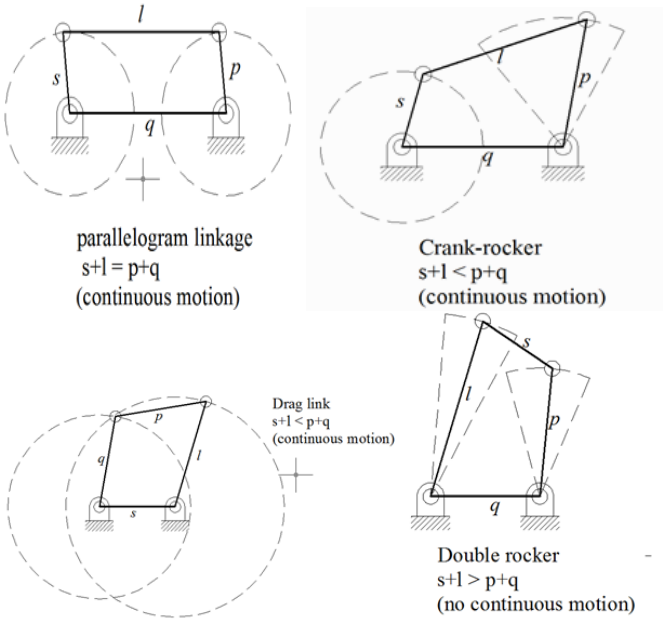

Figure 1. Possible Four bar configurations

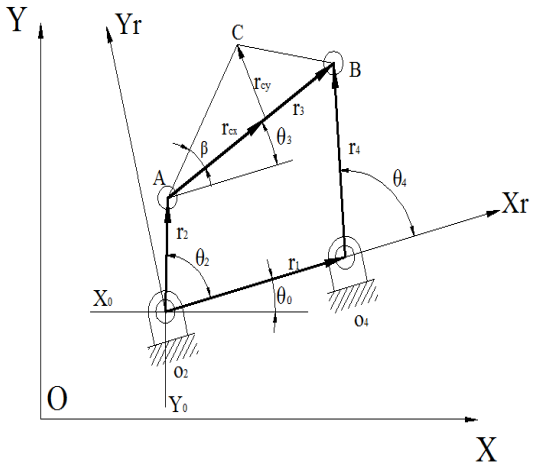

Figure 2. Four bar mechanism in general coordinate system.

K_1, K_2, K_3, K_4 and K_5 are found as;

$$K_1 = \frac{r_1}{r_2}, K_2 = \frac{r_1}{r_4}, K_3 = \frac{r_2^2 - r_3^2 + r_4^2 + r_1^2}{2r_2 r_4}, K_4 = \frac{r_1}{r_3},$$

$$K_5 = \frac{r_4^2 - r_1^2 - r_2^2 - r_3^2}{2r_2 r_3} \quad (6)$$

The angles are then given ;

$$\theta_{3(1,2)} = 2\tan^{-1}\left(\frac{-B \pm \sqrt{B^2 - 4AC}}{2A}\right)$$

$$(7)\ \theta_{4(1,2)} = 2\tan^{-1}\left(\frac{-E \pm \sqrt{E^2 - 4DF}}{2D}\right)$$

(8)

In above equations; ± sign refers to two different configurations of the four bar mechanism. A, B, C, D, E and F expressions are then written as

$$A = \cos\theta_2 - K_1 - K_2\cos\theta_2 + K_3, \quad B = -2\sin\theta_2,$$
$$C = K_1 - (K_2 + 1)\cos\theta_2 + K_5 \quad (9)$$
$$D = \cos\theta_2 - K_1 + K_4\cos\theta_2 + K_5, \quad E = -2\sin\theta_2,$$
$$F = K_1 + (K_4 - 1)\cos\theta_2 + K_5$$

Again referring to Figure 2, the reference frame is taken as $O_2 X_r Y_r$, and the design variables for the mechanism are taken as $r_1, r_2, r_3, r_4, r_5, r_{cx}, r_{cy}, \theta_0, x_0, y_0$. By taking, the coupler position (C) can be written as

$$C_{xr} = r_2\cos\theta_2 + r_{cx}\cos\theta_3 - r_{cy}\sin\theta_3 \quad (10.1)$$

$$C_{yr} = r_2\sin\theta_2 + r_{cx}\sin\theta_3 - r_{cy}\cos\theta_3 \quad (10.2)$$

In previous notation, by taking OXY then;

$$\begin{bmatrix} C_x \\ C_y \end{bmatrix} = \begin{bmatrix} \cos\theta_0 & -\sin\theta_0 \\ \sin\theta_0 & \cos\theta_0 \end{bmatrix}\begin{bmatrix} C_{xr} \\ C_{yr} \end{bmatrix} + \begin{bmatrix} x_0 \\ y_0 \end{bmatrix} \quad (11)$$

Eqn. (11) is later used while performing derivations of the goal function for the mechanism.

5. Optimum Synthesis of Four Bar Mechanism

There is an increase in computer technology which has permitted us in developing routines that apply methods to the minimization of a goal function. There is a common goal function that is the error between the points tracked by the coupler (crank-rocker) and its desired trajectory in general. The aim is to minimize the goal function applying optimization techniques here. Initially the link lengths are chosen according to the Grashof's Theorem. Many cases a continuous rotary input is applied and the mechanism must satisfy the Grashof criteria. The first part computes the position error in the objective function. The sum of the squares of the Euclidean distances between each point is defined and a set of target points indicated by the designer that should be met by the coupler of the mechanism. These points can be written in a world coordinate system as are the target positions on the coupler.

$$C_T^i = \left[C_{xT}^i ; C_{yT}^i\right], \text{ Where i=1, 2, 3,…,n} \quad (12)$$

The variables can be optimized in case of problem without prescribed timing. Structural error is the error between the mathematical function and the actual mechanism. Accordingly, the first part of goal function can be expressed by minimize:

$$f_{obj} = \sum_{i=1}^{N}\left[\left(C_{xT}^i - C_x^i\right)^2 + \left(C_{yT}^i - C_y^i\right)^2\right] \quad (13)$$

N represents the number of points to be synthesized. The geometric magnitudes of four-bar mechanism are previously described in Fig. 2. The design variables and the input angle θ2. The second part of goal function is derived from the constraints which are imposed on the mechanism and set as the following:

(i) The Grashof condition allows for full rotation of at least one link.

(ii) The sequence of input angles, θ_2 can be from the highest to the lowest (or the lowest to the highest).

(iii) The range for the design variables should be given.

(iv) The range of variation for the input angle should be given.

The first three conditions are imposed and the fourth condition is taken as to perform full 360° rotation of the crank in the results presented here. In order to use this definition of the problem when the optimization algorithm is implemented, the constraints are retained and the values are assigned to the design variables X.

6. Case Study on Multiobjective Constrained Optimization

The objective function is constrained one for synthesizing four-bar mechanism. Grashof's condition and constraints regarding to sequential (CW or CCW) rotation of the input crank angle. The constraints play an important role in designing a feasible solution of the mechanism. A high number of initial populations are chosen randomly from the given set of minimum and maximum values of the variables so that a considerable amount of them can play in next iteration. This technique unnecessarily increases CPU time and reverses a large amount of memory in the computer. The refinement of population applied here is only for choosing an initial population and the other part of the evolutionary algorithms

is kept same. The randomly chosen initial population is modified according to feasibility of making an effective mechanism.

In a randomly chosen variable set, the lengths of the linkage and the crank angle, θ2 are taken. The linkage lengths initially chosen as random, that may satisfy the Grashof's condition. The lengths are reassigned if they fail to satisfy this condition. After that randomly chosen, the input angles are rearranged in CW or CCW with randomly choosing first input angle among the initial generated set to meet the constraints. After these modifications in initial population, a comparatively greater number of strings can be found to make a feasible mechanism or the probability of rejection of strings in next iteration is reduced. *fmincon* command is used for nonlinear and many variables. This is a gradient based search function in Matlab© to solve the constraint problem. To run this program and to perform optimization, it is necessary to have a constrained m-file. Firstly the link lengths are defined as r_1, r_2 , r_3, r_4 . The constraints are defined according to the link lengths which is related with the Grashof's Theorem l-the longest link, s-the shortest link, p, q -two intermediate links as l+s<p+q. So the link lengths are chosen according to these values as the constraints. The constraints are set as l=r_1 (the link 1), s=r_2 (the link 2), p=r_3 (the link 3), q=r_4 (the link 4), [30].

6.1. Path generation without timing

Here an example is included to show comparative results on GA and *fmincon*. There are six coupler points required to find out an optimal solution. These points are designed to trace a vertical straight line by changing Y coordinate only. The problem is then defined by;

(i) The design variables are;

$X = \left[r_1, r_2, r_3, r_4, r_{cx}, r_{cy}, \theta_2^i\right]$, Where i=1, 2,…, N and N=6

(ii) Target points are chosen as:

$\left[C_{xT}^i, C_{yT}^i\right] = [(20,20),(20,25),(20,30),(20,35),(20,40),(20,45)]$

(iii) Limits of the variables;

$r_1, r_2, r_3, r_4 \in [13,70]$, $r_{cx}, r_{cy} \in [-60,60]$ and $\theta_2^i \in [0,2\pi]$

where i=1,2,…,N and N=6

(iv) Parameters of GA;

Population Size (PS) = 20, Crossover Possibility (CP) = 0.8, Mutation Possibility-uniform (MP)=0.1, Selection type=Roulette

(v) fmincon conditions;

Maximum iterations= 400

Optimization Toolbox command *fmincon* is compared with GA. The results for GA and *fmincon* are shown in Table 1. Table 2 presents target and traced point with GA. These points are calculated by using Eqns (10.1) and (10.2). Figure 3 shows the target and the traced points in X-Y with GA. Since *fmincon* yields only one result which is included in Table 1 as a separate column. GA results in different values presenting their optimum at the end satisfying the requirement. Table 1 presents 6 precision points on the coupler curve. Objective functions are the same with GA.

6.2. Studying the mechanism with Excel Spread Sheet

All spreadsheet programs are arranged cells as rows and columns; this depends on the requirement given by the user. Here the optimization results are taken and drawn on a spread sheet, Freudenstein's equations are utilized for the synthesis. Initial crank angles are changed successively; different solutions are found and drawn with the mechanism. It is possible to draw coupler curves and its coordinates with velocity and acceleration as well. Then they can be seen on the screen in animated sense. Some study is needed to draw mechanism in Excel. A previously prepared four bar mechanism code has been applied [30]. Fig. 4 shows the four bar mechanism. It is possible to get complete behavior of the mechanism by changing input angle.

Referring to Figure 2, the inputs are given as r1, r2, r3, r4, rcx, rcy and θ2 found from optimization. The mechanism is drawn next. If required, complete kinematic analysis can be seen as positions, velocities and accelerations for each point separately as well.

Table 1. Optimization Results for GA and (fmincon)

			Precision Points				
	[20,20]	**[20,25]**	**[20,30]**	**[20,35]**	**[20,40]**	**[20,45]**	***fmincon***
r_1	56,338	59,97	48,01	52,64	58,90	54,34	40
r_2	54,992	55,01	53,74	59,83	57,40	54,01	50
r_3	55,369	64,89	53,87	50,62	52,06	52,20	50
r_4	54,009	59,87	59,59	57,82	50,56	51,84	60
r_{cx}	0,626	0,69	0,33	0,65	0,113	0,238	32
r_{cy}	0,306	0,33	0,82	0,69	0,206	0,669	0
Θ_2	0,652	0,39	0,52	0,18	0,746	0,498	0,524
f_{obj}	198,1	107,41	66,7	76,05	135,3	244,69	

Table 2. Target and traced points (GA)

POINTS	TARGET-X	TARGET-Y	TRACED-X	TRACED-Y
-20,20	44,011	33,351	41,874	35,997
-20,25	51,965	20,921	52,404	19,529
-20,30	43,839	32,381	41,845	35,122
-20,35	59,472	11,041	59,169	11,311
-20,40	42,753	38,602	44,131	37,07
-20,45	47,869	25,997	47,368	27,398

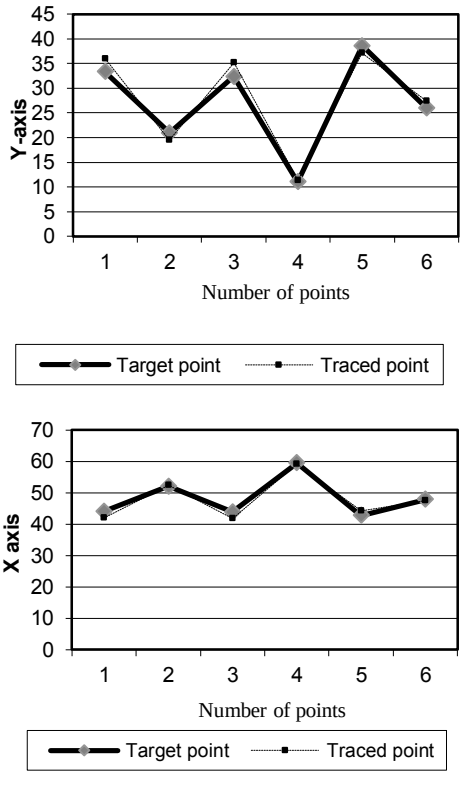

Figure 3. Target and traced points in X-Y with precision points (GA)

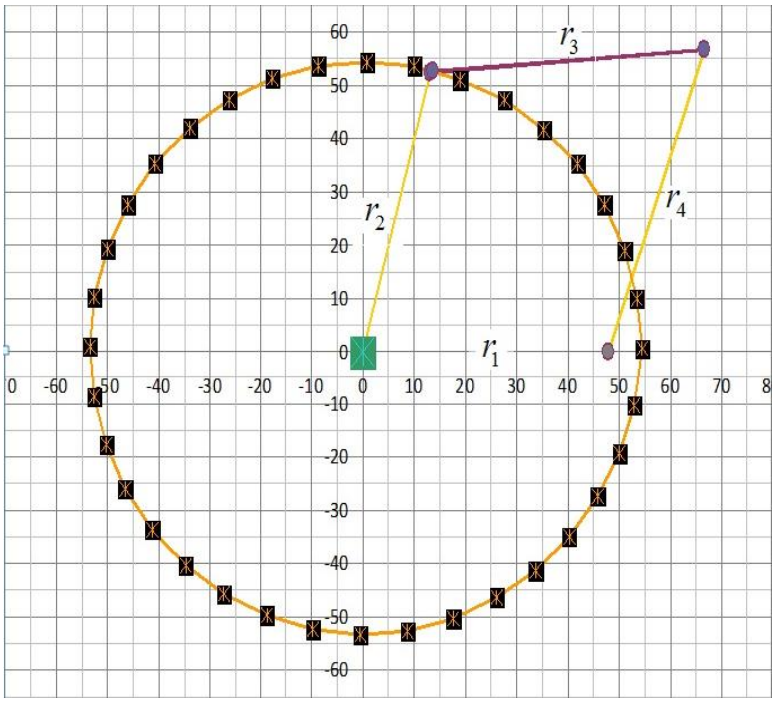

r_1=48.013,r_2=53.745,r_3=53.878,r_4=59.593,r_{cx}=0.332,r_{cy}=0.823

Figure 4. Four Bar Mechanism

7. Conclusion

This has presented a study for synthesis of planar mechanisms; specifically on a one degree of freedom (dof) planar mechanism. The algorithm is developed only for a Grashof's type four bar mechanism. The idea is applicable to all types of planar mechanisms. The only difference will be kinematics analysis of the mechanisms and related constraints. The main advantage seen during implementation is that of simplicity. Utilization of Optimization Toolbox is performed and a fast convergence to optimal solution is observed. Since the routine is performed directly, there will be no need for superior knowledge during optimization. It is seen that use of GA during optimization study is more advantageous to use fmincon. It presents the objective function's optimum each time. The results are similar, but not the same. (Figure 3) Therefore GA toolbox can be easily applied to mechanism synthesis problems. Only problem becomes to derive related kinematics for related mechanism as constraints [30].

References

[1] H. Lipson, 'Evolutionary Synthesis of Kinematic Mechanisms.'Comp. Synt. Lab., Sibley School of Mech. And Aerospace Eng., and Fac. of Computing and Inf. Science, Cornell University, Ithaca, NY-USA, 2000.

[2] J. H. Bickford 'Mechanisms for Intermittent Motion.', Director of production planning, Veeder-Root Company. 'Int. Press Inc., 200 Medison Avenue, N.Y. 10016, 1972.

[3] E.Söylemez, 'Mechanisms', M.E.T.U Mechanical Engineering Department, Publication Number: 64, Ankara.

[4] A. H. Soni, 'Mechanism Synthesis and Analysis.', School of Mechanical and Aerospace Engineering, Oklahoma State University, Stillwater, Oklahoma,

[5] R. N. Norton, 'Design of Machinery-An Introduction to the Synthesis and Analysis of Mechanisms and Machines',McGrawHill–1992.

[6] R. S. Hartenberg, D. J., 'Kinematic Synthesis of Linkages, McGraw Hill-1964.

[7] Y. Lui& J. McPhee, 'Automated Kinematic Synthesis of Planar Mechanisms with Revolute Joints.', System Design Engineering, University of Waterloo, Ontario, Canada.

[8] Ting-YuChen, Chen-MingYang, 'Multidisciplinary design optimization of Mechanisms.', Dept. of Mech. Eng., National Chung Hsing Unv.Taiwan, 25 Oct.2004

[9] T. Back, D. B. Fogel, T. Michalewicz, 'Evolutionary Computation 1- Basic Algorithms and Operators', Taylor and Francis, 2000.

[10] A.E. Eiben, J.E. Smith, 'Introduction to Evolutionary Computing', Springer-Berlin 2003.

[11] R.L. Haupt, S. E. Haupt, 'Practical Genetic Algorithms', 2nd Edition, Wiley-2004.

[12] J.C. Hoskins, Glenn A. Kramer, 'Synthesis of Mechanical Linkages using Artificial Neural Networks and Optimization', IEEE, 1993, 822J-822N.

[13] M.H.F. Dado, Y.S. Mannaa 'An automated procedure for dimensional synthesis of planar mechanisms', J. King Saud Unv., Vol.8, Eng. Sci(1), p.17-41, 1996

[14] R.C. Blackett, 'Optimal Synthesis of Planar Five Link Mechanisms for the Production of Nonlinear Mechanical Advantage', MS Thesis, Virginia Polytechnic Institute, 2001.

[15] P.S. Shiokolas, V. Chandra, J.Kebrle, D. Wilhite, 'Analysis and Simulation for Education using Matlab via the World Wide Web., II Representative Examples- System Simulation and Planar Mechanism Synthesis and Analysis, 109-121, Wiley Periodicals, 2002. [http:/zodhia.uta.edu/development/

[16] J. A. Cabrera, A. Simon, M. Prado, 'Optimal Synthesis of Mechanisms with Genetic Algorithms', Mechanism and Machine theory, 37, 2002, 1165-1177

[17] R. R.Bulatovic, S. R. Djordjevic, 'Optimal Synthesis of a Four Bar Linkage by Method of Controlled Deviation', Theoretical Appl. Mech., Vol.31, No:3-4, pp.264-280, 2004.

[18] M. A. Laribi, A. Mlika, L. Romdhane, S. Zeghloul, 'A Combined Genetic Algorithm-Fuzzy Logic method (GA-FL) in Mechanisms Synthesis', Mechanism and Machine Theory, 39, 2004, p.717-735.

[19] K. G. Cheetancheri, Harry H. Cheng, 'Computer-Aided Analysis of Mechanisms Using Ch Excel', Department of Mech. And Aeronautical Engineering, 2005.
[20] J. F. Collard, P. Fisette, P. Duysinx, 'Optimal Synthesis of Mechanisms using time varying dimensions and natural coordinates', 6th World Congress of Structured and Multidisiplinary Optimization, Rio de Janerio-Brazil, 2005, p.1-10
[21] H.H. Cheng, Dung T. Trang,' Web-Based Interactive Analysis and Animation of Mechanisms', Transactions of the ASME, Journal of Computing and Information Science in Engineering, Vol.6, 2006, 84-90 [http://www.softintegration/webservices/mechanism/]
[22] J. Xie, Y. Chen, 'Application Back Propagation Neural Network to Synthesis of Whole Cycle Motion Generation Mechanism', 12thIFToMM World Congress-Besancon-France, June 18-21, 2007.
[23] Y. Liu, J. McPhee, 'Automated Kinematic Synthesis of Planar Mechanisms with Revolute Joints', Mechanics Based Design of Structures and Machines, 35, p.405-445, 2007.
[24] S. Erkaya, İ. Uzmay, 'A Neural-Genetic (NN-GA) approach for optimizing mechanisms having joints with clearance', Multibody System Dynamics, 20, 2008, 69-83.
[25] N. N. Zadeh, M. Felezi, A. Jamali, M. Ganji, 'Pare to optimal Synthesis of four-bar mechanisms for path generation', Mechanism and Machine Theory, 22, 2009, 180-191.
[26] S. K. Archaryya, M. Mandal, 'Performance of EAs for four-bar linkage synthesis', Mechanism and Machine Theory, 44, 2009, 1784-1794.
[27] A. Kentli, A. K. Kar, E. Taçgın, 'Genetic Coding Application to Synthesis of Planar Mechanisms', 5th. Int. Adv. Tech. Symp. (IATS'09), May 13-15, 2009, Karabük-Türkiye.
[28] K. Sedlaczek, P. Eberhard, 'Augmented Lagrangian Particle Swarm Optimization in Mechanism Design', Journal of System Design and Dynamics, 410-421. [www.itm.uni-stuttgart.de{research/alpso]
[29] F.Penunuri, R.P. Escalante, C. Villanueva, D. Pech-Oy, 'Optimum Synthesis of Mechanism for single and hybrid task using differential evolution', Mechanism and Machine Theory, Vol.46, No.10, p. 1335-1349, 2011.
[30] H. Erdoğan, 'Synthesis of Planar Mechanisms using Evolutionary Algorithms', Gaziantep University, Ms. Thesis, September 2011.